

Challenges, Solutions and Lessons Learnt from Testing Power System Performance with a General Power Theory-Controlled Converter

Pitambar Jankee
Department of Electrical
Engineering
University of Cape Town
Cape Town, South Africa
jnkpit001@myuct.ac.za

Charles Trevor Gaunt
Department of Electrical
Engineering
University of Cape Town
Cape Town, South Africa
ct.gaunt@uct.ac.za

Michel Malengret
Department of Electrical
Engineering
University of Cape Town
Cape Town, South Africa
michel.malengret@uct.ac.za

Ibrahim Abdulhadi
Power Networks Demonstration
Centre
University of Strathclyde
Glasgow, United Kingdom
ibrahim.f.abdulahadi@strath.ac.uk

Behnam Feizifar
Power Networks Demonstration Centre
University of Strathclyde
Glasgow, United Kingdom
behnam.feizifar@strath.ac.uk

Zhiwang Feng
Institute for Energy and Environment
University of Strathclyde
Glasgow, United Kingdom
zhiwang.feng@strath.ac.uk

Graeme Burt
Institute for Energy and Environment
University of Strathclyde
Glasgow, United Kingdom
graeme.burt@strath.ac.uk

Abstract—A novel control approach for power-electronic converters has been shown to reduce the losses in delivery systems to below the levels possible with conventional methods. In this research, an 80 kW converter was retrofitted to operate using the General Power Theory (GPT). The effect of compensation using the GPT in a three-bus test network was studied by Simulink simulation and in the physical power system infrastructure of the Power Networks Demonstration Centre. The simulation results demonstrated that the converter did not need the concept of reactive power for control and could improve the system power factor. The experimental measurements were used for comparison with the simulation results. Challenges faced during experimental testing are discussed. Solutions are proposed to resolve some of the measurement problems that hindered the full experimental validation at this stage. The practical lessons learnt are helpful for future tests and identified real-world issues that may be encountered during deployment.

Keywords—control, converter, efficiency, loss, measurement, physical testing, power theory

I. INTRODUCTION

A radically new approach to define power and minimise losses in power systems was published in 2020 [1]. It extended an earlier time-domain approach [2, 3] to the frequency domain. The theory is referred to as the General Power Theory (GPT) because it applies consistently to power systems with any number of wires, with unbalanced voltages, currents, or delivery system impedances, harmonic distortion, and frequency-dependent impedances. The GPT challenges 100-year-old power theories and most conventional approaches that are based on a measurement model that neglects unbalance, distortion, and the delivery system.

This work was supported in part by a UCT Innovation Builder grant IB21-011, Ario MeTaPower, and the European Union's Horizon 2020 research and innovation program under grant agreement No 870620 in the ERIGrid 2.0 project.

The minimisation of delivery system losses is inherent in the derivation and rigorous mathematical formulation of the GPT [1]. Since it was published, it has been tested using Electromagnetic Transients (EMT) simulations of power systems to investigate the effects of harmonic distortion in unbalanced feeders [4, 5], and voltage drop caused by geomagnetically induced currents during solar disturbances [6].

The GPT's minimisation of losses by identifying the unique optimum current components delivering power to a load, or injecting power from distributed sources, suggests a practical and direct application of the theory to power-electronic converter control. A GPT-controlled compensator operating in the natural (abc) reference frame should be able to reduce the losses in a power system below the levels achieved by conventional approaches which use Clarke's or Park's reference frame transforms to determine the reference currents to be injected by the compensator.

To test this hypothesis and win acceptance of the novel converter control approach, the validity of the GPT needs to be tested in a physical power system. This paper describes the simulations and the physical experimental tests of a small power system with an 80 kW 3-phase 3-wire converter operating as a compensator. The emphasis is on the delivery losses and power factor in a simple feeder as indicators of the delivery efficiency gained by GPT control. The study is part of the Transnational Lab Access program in the ERIGrid 2.0 project [7].

II. DEFINING POWER QUANTITIES

A. Conventional Power Theories

Many concept models, theories, and definitions of electric power have been proposed during the past 130 years. Most

models are based on mathematics but lack a solid physics foundation and make assumptions that are violated in practical systems. Only a few power theories define the components of power in the context of a power system. For example, most conventional power definitions use the concept of reactive power which is defined assuming an impedance-less delivery system such that the source voltage is equal to the point of connection (PoC) voltage. This ideal condition never occurs in practice. Current through the delivery resistance causes voltage drop along the feeder and through the reactance causes voltage rotation. Assuming the source voltage is equal to the PoC voltage to define power terms without losses cannot provide a physical interpretation of the system performance. Some issues with the reactive power definition have been identified and discussed in [8].

In practical power systems, voltages and currents are typically unbalanced and distorted, but these effects are neglected in most definitions, studies, and metering. When unbalance and distortion are omitted from the analysis, the measurement uncertainty is unknowable without having a more representative model for comparison.

There are practical implications of the inadequacies of conventional power theory in the presence of unbalance and waveform distortion. The multiple inconsistent definitions of power components (apparent and reactive power, and power factor) lead to different measurement results [9] and disputes with customers [10].

B. Industry Standards

Most electrical standards such as the IEEE 1459 standard [11] and IEC 131-11-44 [12] define power components for an apparatus, which is for a device or an assembly of circuit elements comprising a load. Industry standards use the concept of the power triangle assuming orthogonality between the real power P and reactive power Q . This orthogonal relationship may not be valid under conditions of unbalance and harmonic distortion [13].

Power-electronic converters are designed and controlled to limit the harmonic power exported to the grid. The IEEE 519 standard [14] for power quality governs acceptable harmonic levels for any apparatus connected at a PoC. However, minimum loss in a power system can only be achieved by controlling harmonic power flow. Therefore, a converter designed according to the limits imposed by the IEEE 519 standard may not achieve minimum loss operation.

C. General Power Theory

The GPT [1] establishes the equations for measurement and control at the PoC of a load, generator, or other network. The only inputs required are the measurements of voltage, current, and Thévenin-Equivalent Impedance (TEI) of the delivery system made at the PoC.

An important outcome of the physics-consistent model and algebraic rigour of the GPT is that no parameter of reactive power or non-active component orthogonal to the active power measured at a PoC (incurring delivery loss but not contributing to power delivery) can be identified. Thus, analysis incorporating Q in conventional power theory can only

approximate the physical behaviour of power systems and reactive power compensation.

EMT simulations demonstrated the validity of the GPT but simulations rely on assumptions, approximations, embedded models, and simplifications, which can introduce inaccuracies in the results. Therefore, simulations alone cannot fully validate and establish the feasibility of the novel ideas. The integration of physical hardware testing in a real-world environment is an imperative step in the innovation process.

Controller Hardware-In-the-Loop (CHIL) and Power Hardware-In-the-Loop (PHIL) tests are increasingly used for the functional testing of system components by connecting the hardware to real-time simulators of the network to which the equipment is connected. Given the increasing complexity of inverter dominated systems and the emergence of subtle transient behaviours, care must be taken to use appropriate HIL methods and validate these against physical infrastructures and grid deployments [15].

III. TESTING POWER SYSTEM PERFORMANCE USING THE GPT

The objective of the tests was to demonstrate the effects on power systems of a converter operating under GPT control. The converter used for the experiments was a commercial unit supplied by Ario MeTaPower, an inverter manufacturing company in Pretoria, South Africa. It is rated 80 kW at 400 V and can operate as a compensator with zero average energy import/export over a cycle or as an inverter injecting power into the delivery system. It used a conventional dq0-based controller and was retrofitted with GPT-control that defines the output currents required for optimal delivery system performance [16].

To obtain a reliable assessment of the effects of applying GPT-control, it was necessary to test the converter in a physical “real-world” environment. The facilities at Strathclyde University’s Dynamic Power Systems Laboratory (DPSL) and Power Networks Demonstration Centre (PNDC), which offer funded access as part of the ERIGrid 2.0 collaboration [7], were chosen for their configurable network topologies and instrumentation. Before despatch, preliminary tests had been carried out with an isolated grid emulator and with the converter connected to the South African national grid [16].

The objective was to compare Power Hardware In the Loop (PHIL) simulations at DPSL with test results from the physical experiments at PNDC, and with the results of EMT simulations, to guide further simulations of other cases, and refine control techniques used in simulations or on actual converters.

A. Test Network

Fig.1 shows the single line diagram of the test network used at PNDC and images of the physical equipment. The network was reconfigured to a three-phase, three-wire power system. The whole network’s infeed is supplied by a local distribution network operator (DNO). A 2 MVA 11/11 kV Dyn11 isolation transformer supplies the primary switchboard (SWB), a 130 m MV feeder designed using 11 kV, 95 mm² copper XLPE cables (MV-007 and MV-013), and a mock impedance unit (MIU1). The MV feeder supplies a 315 kVA, 11/0.433 kV, Dyn11 transformer (GMU-A) and an LV cable to a test bay F2, which is bus 1 of the test installation. The 185 mm² copper XLPE LV

cables sections from bus 1 are labelled on Fig. 1. Buses 1 and 2 are connected by 260 m of LV cables, buses 2 and 3 are connected by 455 m of cables, and more cables connect the load banks LB1 to LB4, shown in green, to bus 3. The test feeder is also suitable for other experiments with the converter operating as an inverter at bus 3 supplying energy to a load at bus 2.

A regenerative three-phase load emulator was connected to test bay F1 at bus 2. It could act both as a current source and/or current sink at selected harmonics. In some tests, the load emulator was moved to test bay D1, downstream from bus 3. All loads downstream of bus 3 are treated as a lumped load.

Unbalance can be introduced by changing the load bank configurations or using the regenerative load emulator capable of simultaneously drawing or injecting currents. Harmonics can also be injected or drawn using the load emulator. At F1/bus 2 it introduces distortion to the delivery systems, and at D1/bus 3 it distorts the load currents.

The GPT-controlled compensator was connected to test bay D1 at bus 3. The dc-bus of the converter was supplied by two parallel 18 kW, 400 V dc-power supplies fed from an auxiliary supply.

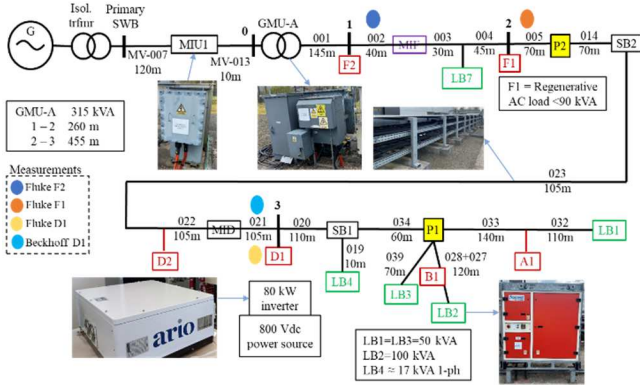


Fig. 1. The single line diagram of test network setup at PNDC.

LV and MV network diagrams and fault levels were provided by PNDC. Cable datasheets including lengths were provided for determining the TEI of the network, which is an input to the calculation of compensating currents using the GPT approach. The parameters were also used to develop a simulation model of the network. The TEI from the equivalent source to D1/bus 3 was calculated to be $R_{th} = 0.1741 \Omega/\text{phase}$ and $X_{th_{50\text{Hz}}} = 0.09954 \Omega/\text{phase}$. The simplified equivalent circuit of the test network is shown in Fig. 2.

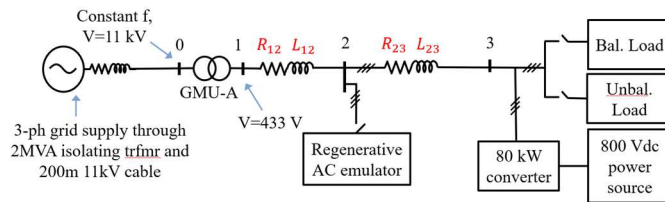


Fig. 2. Equivalent circuit of the delivery system and test feeder from the Thévenin equivalent source to the compensator at the PoC of Bus 3.

B. Instrumentation

Two Fluke 430 Series II Power Quality and Energy Analysers were used to collect feeder measurements at buses 1 and 2, and a Beckhoff Data Acquisition (DAQ) system at bus 3. A third Fluke Analyser measured the converter currents at bus 3. The position of each meter within the test network is shown in Fig. 1.

The Fluke meters are equipped with in-built calculations of root mean square (rms) values, Total Harmonic Distortion (THD), harmonic spectrum, and statistical data representation amongst other functionalities. However, the calculation steps are not specified in the Fluke meter's user guide. Therefore, it was preferred to extract instantaneous values of currents and voltages measured by each Fluke meter and post-process the data to analyse the results. The Fluke meter exports data as a .txt file delimited using a tab. For each test case, measurement data was stored on a detachable SD card on the Fluke meter and the .txt file was renamed by assigning a measurement number. The measured data was then copied to a laptop for analysis using PowerLog software and MATLAB Simulink.

Measurements at test bay D1 (feeder input to bus 3) were made using the Beckhoff DAQ and observed in the Beckhoff software on a dedicated laptop. The Beckhoff DAQ was chosen instead of the Fluke meters since the former can measure at a fixed sampling frequency of 5 kHz. Data from the Beckhoff DAQ can be exported in different formats. A csv file was preferred in this case as data in a csv file can easily be imported onto MATLAB. The measured data (V_{AB} , V_{BC} , V_{CA} , I_A , I_B , I_C) was then transferred to a USB flash memory and imported on a laptop. A MATLAB script was developed which reads data from the .csv files exported and generates a timeseries for each measured quantity. A Simulink model was then developed which imports the generated timeseries and implements a Discrete Fourier Transform (DFT) algorithm. The complex rms (crms) values of currents and voltages including their angles with respect to a voltage reference phasor were then used as inputs to a GPT spreadsheet. The outputs were the crms values of compensating currents including their angles referenced to the voltage reference. The values of the compensating currents were entered manually in the code of the converter controller. This was achieved using Code Composer Studio.

C. Simulations

Models of the test networks were developed in Simulink and RSCAD. They were tested using a different converter in the DPSL [17] microgrid, under a variety of different network conditions. In this paper, an example showing GPT compensation for an unbalanced resistive and inductive load is shown. A balanced three-phase 50 kVA constant impedance load with an impedance factor R/Z of 0.85 was modelled. To generate the unbalance, a 17 kVA load with $R/Z=0.85$ was connected between wire 1 and wire 2.

D. Experimental Test

Once suitable results of load current and feeder voltage drop were obtained from Simulink simulations, the same test network was set up at PNDC and the effects of GPT compensation using the 80 kW converter were investigated.

The base case voltages and currents upstream the PoC were measured (before compensation condition). The GPT reference currents were set on the converter and injected at the PoC. Measurements were taken (during compensation condition). The compensator was then switched off to return to the base case and measurements taken again (after compensation condition).

IV. POST-PROCESSING OF MEASURED DATA FROM EXPERIMENTAL TESTS

A. Fluke Meter

A limitation was identified in the Fluke meter in that its data sampling rate in “PowerWave” data capture mode is variable. There are random occurrences of the same timestamp, and multiple values of the measured quantity are associated with each timestamp.

Date	Time	AB(V)	BC(V)	CA(V)	A(A)	B(A)	C(A)
2023/05/04	11:00:07.947	-282.428	595.456	-312.985	42.992	-43.449	0.876
2023/05/04	11:00:07.947	-320.451	595.499	-275.005	45.052	-40.703	-4.654
2023/05/04	11:00:07.948	-360.884	591.917	-231.070	46.425	-37.689	-9.041
2023/05/04	11:00:07.948	-400.467	595.702	-185.193	47.684	-35.515	-12.512
2023/05/04	11:00:07.948	-438.705	578.581	-139.876	49.477	-33.264	-16.518
2023/05/04	11:00:07.948	-474.181	567.964	-93.783	50.392	-29.259	-21.400
2023/05/04	11:00:07.949	-503.917	548.888	-44.928	50.545	-23.956	-26.855
2023/05/04	11:00:07.949	-527.741	521.526	6.172 50.392	-18.883	-21.815	
2023/05/04	11:00:07.949	-546.083	487.776	58.307	49.858	-15.450	-34.676
2023/05/04	11:00:07.949	-560.843	451.782	109.061	49.515	-13.008	-36.697
2023/05/04	11:00:07.950	-572.712	413.673	159.039	48.676	-9.689	-39.177
2023/05/04	11:00:07.950	-580.912	372.932	207.937	47.112	-5.684	-41.580
2023/05/04	11:00:07.950	-584.925	334.477	250.405	45.815	-2.213	-43.678
2023/05/04	11:00:07.950	-560.843	451.782	109.061	49.515	-13.008	-36.697
2023/05/04	11:00:07.951	-585.781	291.794	294.944	44.022	2.022	-46.158
2023/05/04	11:00:07.951	-586.436	249.585	336.851	41.389	6.638	-48.065
2023/05/04	11:00:07.951	-582.293	204.700	377.593	38.452	10.567	-49.019
2023/05/04	11:00:07.951	-575.690	158.780	416.910	36.087	13.924	-50.011
2023/05/04	11:00:07.952	-567.360	113.377	453.940	33.264	18.501	-51.651
2023/05/04	11:00:07.952	-554.110	65.730	488.380	28.915	23.537	-52.376
2023/05/04	11:00:07.952	-531.797	14.890	516.865	23.689	27.962	-51.498
2023/05/04	11:00:07.952	-502.018	-36.124	538.142	19.417	31.929	-50.089
2023/05/04	11:00:07.953	-468.009	-88.345	556.596	16.174	34.856	-50.556
2023/05/04	11:00:07.953	-430.677	-140.222	570.942	13.046	36.697	-49.477
2023/05/04	11:00:07.953	-391.101	-180.602	579.703	9.613 39.063	-48.447	
2023/05/04	11:00:07.953	-350.101	-236.206	586.307	5.836 41.809	-47.417	

Fig. 3. Sample .txt file produced using the export function from the Fluke meters. The data pro-cessing revealed irregular instances where a single timestamp appears multiple times, and each timestamp is associated with multiple values of the measured quantity.

To address this issue, a MATLAB script was developed to read data in the .txt files from all Fluke meters and generate a separate variable for the measurement timestamp, voltages, and currents. The measurement timestamps are converted into a time axis in seconds. Then, the script finds data points representing identical times in seconds and generates a new time axis with no repeated time data. For each set of identical time points, the corresponding set of voltage or current measurements is generated and their average calculated. Next, the original measured voltages and currents are replaced with their average values. The new post-processed data is upsampled to a fixed 5 kHz sampling frequency and a timeseries is generated for the upsampled data to represent each measured quantity.

Fig. 4 shows an example of the results obtained after post-processing the exported data from one of the Fluke meters. The original exported voltage data distorts the waveform because multiple values of the measured quantity are associated with each timestamp. The post-processed data is more useful for analysing the voltages and currents as it produces smooth waveforms. Note that the distortion introduced by the post-processing approach was negligible when comparing the individual harmonics on the Fluke meter and those calculated from the post-processed data.

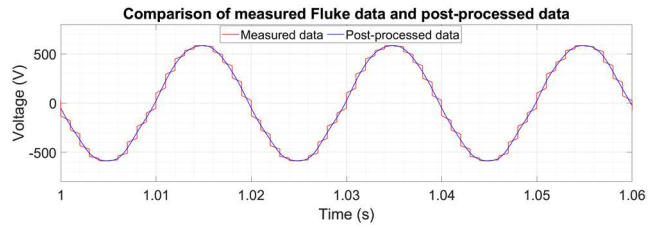


Fig. 4. Comparison of measured Fluke data and up-sampled data after post-processing using developed MATLAB script.

B. Beckhoff DAQ System

Plotting the time series Beckhoff data revealed that it captured outliers in the measurement data. These outliers distorted the waveshape of measured currents and voltages. Therefore, to remove the outliers from each measured quantity, a MATLAB script was developed which identifies the outliers in the measured data using a moving window with median filtering. A spline interpolation then replaces the outliers in the data.

Fig. 5 shows an example of the outliers measured and removed in the measured data. The outliers were removed and replaced after post-processing the measured data using the developed MATLAB script. The interpolation technique avoids distortion in the waveforms and maintains the trend in the waveshape. This was an important step before analysing the results from the Beckhoff measurement.

The post-processing also revealed a frequency drift in the Beckhoff measurement which had to be corrected for each identified time interval used for analysis. An approach of identifying six 250-cycle periods before and after the end of compensation was used, in both Fluke and Beckhoff measured voltages. The ratio between the time periods identified on the Beckhoff to the time periods identified on the Fluke gave an indication of the timer drift which was found to be slow and small enough to be corrected by matching the waveforms of the common voltages or currents from different meters.

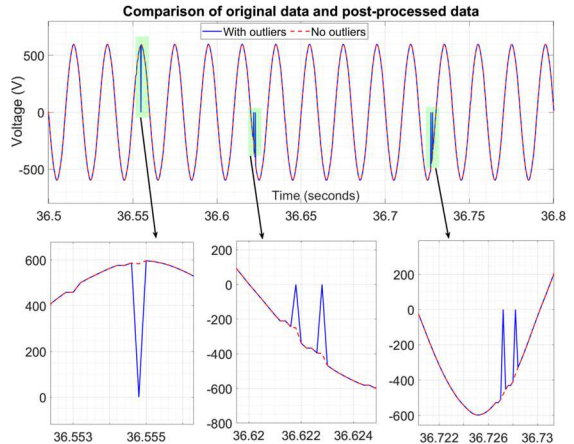


Fig. 5. Comparison of original Beckhoff data with outliers and post-processed data after removing outliers

C. Time-Synchronisation of Fluke and Beckhoff Measurements

Simulations using MATLAB Simulink have shown that the cable capacitance had negligible effect on the network

response. Since the network was modelled as a radial feeder with no intermediate load at bus 2, the same currents flow from bus 1 to bus 3. In other words, the current measured in each wire by Fluke meters F1 and F2 and Beckhoff measurement D1 must be equal. Therefore, Beckhoff D1 currents were used to synchronise with the Fluke meters F1 and F2 before, with, and after compensation currents flowed.

Moreover, Fluke D1 and Beckhoff D1 at bus 3 measured the same three-phase voltages. Time-synchronisation of the Fluke D1 and Beckhoff D1 measurements was achieved by matching their voltages.

Note that when synchronising the currents and voltages, four time intervals were identified representing a “before compensation” (t1), two “during compensation” (t2 and t3), and an “after compensation” (t4) conditions. Using Beckhoff D1 as the reference measurement, the corresponding time shifts applicable to all Fluke meters during each time interval were determined by matching the positive-going zero crossing of either currents or voltages.

Fig. 6 shows an example of synchronised Beckhoff D1, Fluke F2 and F1 measurements during two of the chosen time intervals for synchronisation, at the transition from ‘during’ to ‘after’ compensation. The results proved that the time synchronisation method was effective in resolving the measurement problems identified in section IV (B).

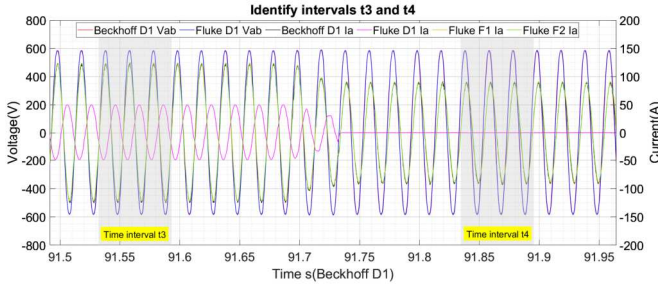


Fig. 6. Synchronised Beckhoff D1 and Fluke voltages and currents after zero-crossing matching.

V. RESULTS

A. Simulation

Fig. 7 shows the PoC currents and voltages measured from the common reference point (wire 1 or phase A). Table I provides a summary of the power, loss, percentage voltage unbalance as per the ANSI/NEMA definition [18] and the power factor defined using the conventional power triangle approach and the GPT.

The voltages and currents were unbalanced before compensation. The voltage unbalance was 1.8680 %. GPT compensation reduced the unbalance to 0.1738 % and compensated for the avoidable power loss. The system power factor defined by the GPT improved from 0.8094 to 0.8751. The conventional power factor defined without reference to the delivery system improved from 0.8276 to 0.9995. The results show that an improvement in the power delivery can be achieved without the need to use reactive power as a control parameter.

Since the load was modelled as a constant impedance, compensation increased the PoC voltage resulting in higher power consumed by the load. However, the percentage loss relative to the load power dropped during compensation as expected. If the load was a constant power load, then the loss in the system for the *same* power delivered to the load would be minimal.

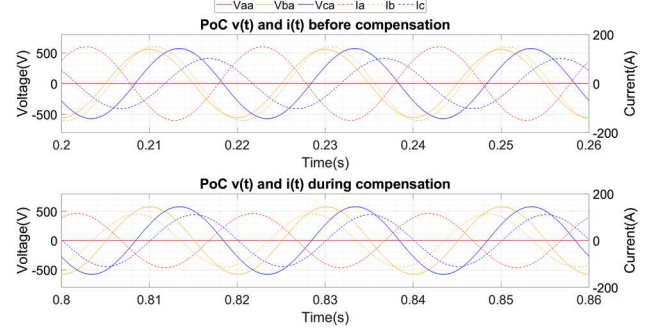


Fig. 7. Simulation results showing the effects of GPT compensation for an unbalanced resistive inductive load.

TABLE I. POWER, LOSS AND POWER FACTOR BEFORE AND DURING COMPENSATION

Quantity	Before comp	During comp
PoC power [W]	55231.64	56564.09
Loss [W]	4832.00	2178.03
% loss	8.75	3.85
% Unbalance	1.8680	0.1738
Conv. PF	0.8276	0.9995
GPT PF	0.8094	0.8751

B. Lab Testing

Using post-processed voltages and currents for one of the experimental tests conducted at PNDC, the fundamental frequency power, loss and apparent resistance of the cables were calculated as shown in Table II.

TABLE II. FUNDAMENTAL FREQUENCY POWER MEASUREMENTS AND DERIVED RESISTANCES R_{1-2} AND R_{2-3}

Quantity	At t1 (before comp.)	At t2 (during comp.)	At t3 (during comp.)	At t4 (after comp.)
P_1 [W]	47090.30	60058.53	60060.52	47125.18
P_2 [W]	46937.98	59840.40	59897.98	46946.91
P_3 [W]	46189.77	55736.53	55961.84	46214.66
Loss P_{1-2} [W]	152.32	218.13	162.54	178.27
Loss P_{2-3} [W]	748.21	4103.87	3936.14	732.25
R_{1-2} [Ω /100m]	0.010945	0.008560	0.006373	0.012792
R_{2-3} [Ω /100m]	0.013606	0.040644	0.038904	0.013316

Despite meticulous synchronisation of the data collected, a reality check of the currents and power measured during four 3-cycle periods at each bus gave inconsistent estimates of the resistance of each of the two branches 1-2 and 2-3 (See Fig. 2) before, during, and after the converter currents were injected at Bus 3. The discrepancy in the difference in power between bus bars and the I^2R loss in constant resistance cables could not be resolved and made interpretation of the measurements impossible.

C. Lessons Learnt during Experimental Testing

The nature of the tests carried out in this project differs from most physical testing of apparatus and control systems. Some of the valuable lessons gleaned from them are described below.

- In these tests, the item under test is the power system itself. It is impossible to measure and control the whole system and is necessary to treat it as represented by its frequency-dependent, varying equivalent impedances.
- The test arrangement and protocol must have ways of confirming the physical credibility of the results and, possibly, use check-metering.
- The base case introduces its own distortion and unbalance, which are usually neglected in simulations.
- The inability of predicting or controlling the voltage sensitivity of all loads on the power system to the change in voltage caused by compensation or inverter control is usually neglected. The tests showed these can be significant. Practical inverters and compensators will need responsive control to maintain optimal control of delivery losses continuously.
- Even in experimental testing, it is possible to set up non-physical conditions. For example, the phase angles of currents injected or drawn by a load emulator may not be representative of real physical equipment like rectifiers and saturated transformers.
- It is recommended to capture instantaneous values of currents and voltages, and post-process the data using mathematical approaches that do not have underlying assumptions embedded in operational measurements. Most meters provide power measurements calculated using a specific power theory. These calculated parameters may not be physically correct and may be misleading in terms of actual system performance.
- Special care needs taken in selecting meters with appropriate waveform capture modes. Fluke meters use a variable sampling frequency which may be complex to post-process especially when required to perform Fast Fourier Transform (FFT) of waveforms.
- Frequency drifts may appear in measurement data due to incorrect timer settings. Such data requires careful post-processing and synchronisation, if required.

VI. CONCLUSIONS

In the dynamic and evolving field of modern power systems, the validation of novel concepts is a critical step towards understanding physically interpretable network responses. Simulation results have shown that power delivery efficiency can be improved without the need for reactive power. While simulations are valuable for preliminary investigations, they fall short in providing a complete and reliable validation process. The incorporation of physical infrastructure testing is essential for verifying assumptions, detecting unforeseen challenges, quantitatively evaluating performance, and validating scalability. The experience reported in this paper demonstrates some of the practical issues that may arise during such testing, and shares some of the mitigating measures required to avoid inconsistent and physically uninterpretable

results. This validation exercise has given valuable insight of the proposed control method, has informed areas of further investigation and validation approaches that may be relevant to other innovative converter control programmes.

ACKNOWLEDGMENTS

We thank Mr. Alastair Wilson for setting up the test network and Ario MeTaPower for providing the 80 kW converter.

REFERENCES

- [1] M. Malengret and C. T. Gaunt, "Active Currents, Power Factor, and Apparent Power for Practical Power Delivery Systems," *IEEE Access*, vol. 8, pp. 133095-133113, 2020, doi: 10.1109/ACCESS.2020.3010638.
- [2] M. Malengret and C. T. Gaunt, "General theory of instantaneous power for multi-phase systems with distortion, unbalance and direct current components," *Electric Power Systems Research*, vol. 81, pp. 1897-1904, October 2011.
- [3] M. Malengret and C. T. Gaunt, "General theory of average power for multi-phase systems with distortion, unbalance and direct current components," *Electric Power Systems Research*, vol. 84, pp. 224-230, March 2012.
- [4] P. Jankee, D. T. O. Oyedokun, H. K. Chisepo, "Network Unbalance Compensation Comparison: Conventional pq Theory vs the General Power Theory," in 2022 IEEE PES/IAS PowerAfrica, Kigali, Rwanda, 2022, pp. 1-5.
- [5] H. K. Chisepo and C. T. Gaunt, "Towards Asymmetrical Modelling of Voltage Stability in the Presence of GICs," in 2022 IEEE PES/IAS PowerAfrica, Kigali, Rwanda, 2022, pp. 1-5.
- [6] H. K. Chisepo, C. T. Gaunt, P. Jankee, "Applying and comparing the general power theory compensation for unbalance and harmonics," in 2022 57th International Universities Power Engineering Conference (UPEC), Istanbul, Turkey, 2022, pp. 1-6.
- [7] <https://erigrad2.eu/lab-access/> (accessed May. 01, 2023).
- [8] C.T. Gaunt and P. Jankee, "Is reactive power a zero quantity?" *IEEE W'shop on Applied Measurements for Power Systems (AMPS)*, Bern, 2023, in press.
- [9] NEMA (2011). Definitions for Calculations of VA, VAh, VAR, and VARh for Poly-Phase Electricity Meters. NEMA C12.24 TR-2011, National Electrical Manufacturers Association, Rosslyn, VA, USA, 2011.
- [10] Berrisford, A.J. (2012). Smart meters should be smarter. *IEEE Power and Energy Society General Meeting*, San Diego, USA, <https://doi.org/10.1109/PESGM.2012.6345146>.
- [11] Standard definitions for the measurement of electric power quantities under sinusoidal, non-sinusoidal, balanced, or unbalanced conditions, *IEEE Standard 1459-2010*.
- [12] IECV, International Electrotechnical Vocabulary, International Electrotechnical Commission, <https://www.electropedia.org/>.
- [13] D. Oyedokun, P. Jankee, M. Soltanian and H. Chisepo, "Analysis and Compensation of Power Systems with Harmonics and Unbalance," 2023 31st Southern African Universities Power Engineering Conference (SAUPEC). Johannesburg, South Africa, 2023, pp. 1-5, doi: 10.1109/SAUPEC57889.2023.10057672.
- [14] IEEE Standard for Harmonic Control in Electric Power Systems, *IEEE Std 519-2022*.
- [15] A. Alassi, Z. Feng, K. Ahmed, M. Syed, A. Egea-Alvarez, and C. Foote, "Grid-forming VSM control for black-start applications with experimental PHIL validation," *International Journal of Electrical Power & Energy Systems*, vol. 151, p. 109119, 2023.
- [16] P. Jankee, L. Schmidt, C.T. Gaunt, M. Malengret, K. Litsoane, R. Yorke, "Design, performance and testing of a converter under General Power Theory control," *Cigre Southern Africa Regional Conf.*, 2023, in press.
- [17] C. T. Gaunt, P. Jankee, Z. Feng, G. Burt, Experimental validation of the General Power Theory using Power-Hardware in the Loop - opportunities for new converter controls. (Unpublished).
- [18] Motors and Generators, *ANSI/NEMA Standard MG1-1993*